Miscibility of oligomeric poly(dimethyl siloxanes) with long-chain unbranched alkanes: 2. Unsymmetrical cloud point curves

Malcolm B. Huglin and Ibrahim Mohd. Idris
Department of Chemistry and Applied Chemistry, University of Salford, Salford M5 4WT, UK

(Received 16 February 1983)

Previously obtained cloud point curves for mixtures of oligomeric poly(dimethyl siloxanes) (weight fraction W_1) with oligomeric polyethylenes have been supplemented by the use of samples of higher molecular weight. Initial flat regions at low–medium W_1 as well as a slight shoulder at extremely high W_1 are now considered to be due to crystallization, since the temperatures at which they occur are the melting points of the oligoethylenes. The actual cloud point curves were of an unsymmetrical dome shape, the form of which could not be simulated by using a concentration-independent interaction parameter g in the Flory–Huggins equation. However, spinodals calculated by assuming a quadratic dependence of g on composition were of the same shape as the experimental cloud point curves. The critical compositions calculated on this basis were also close to the experimental ones.

Keywords Poly(dimethyl siloxanes); polyethylene; cloud point curve; spinodal; interaction parameter; crystallization

INTRODUCTION

In part 1[1] of this series, observations were reported on the miscibility of several low molecular weight samples ($\bar{M}_n = 481$–$1430\,\mathrm{g\,mol^{-1}}$) of poly(dimethyl siloxane) with low molecular weight species of polyethylene (n-alkanes of $M = 254$–$618\,\mathrm{g\,mol^{-1}}$). This study as a model for polymer–polymer compatibility is extended here by the use of oligomers of higher molecular weight. The nomenclature is also systematized as follows.

Oligomers of poly(dimethyl siloxane) are denoted as OSm_1 and those of polyethylene as OEm_2, where m_1 and m_2 are respectively the nearest integral values of the number average chain lengths. For the OSm_1 series the trimethyl silyl end groups were discounted and m_1 obtained by dividing the molecular weight by that of the repeating unit, $-\mathrm{Si(CH_3)_2{-}O}-$. The terminal methyl groups were discounted for the OEm_2 series and m_2 obtained by dividing the molecular weight by that of the repeating unit, $-\mathrm{CH_2{-}CH_2}-$. For example, the smallest oligomer of poly(dimethyl siloxane) used has $\bar{M}_n = 481\,\mathrm{g\,mol^{-1}}$ and this is denoted accordingly as OS4. Similarly, $\bar{M}_n = 2031$ for the largest polyethylene used and this is denoted as OE73. The composition of mixtures is expressed as the weight fraction W_1 of OSm_1.

EXPERIMENTAL

Materials

The source of mode of isolation for some of the oligomers used has been described elsewhere[1,2] and mention is made here of the new samples only. With regard to OS31, which was isolated by vacuum distillation (1 mmHg pressure) of a commercial sample DC 200/20 (Hopkin and Williams), the deposition of white crystals in the condenser was noted at high temperature (> 583K). These were shown by g.p.c. to be cyclic oligomer, which was present partially also in the liquid distillate[1] (we are much indebted to Drs K. Dodgson and J. A. Semlyen of the University of York, UK, for these analyses). Several washings of the distillate with acetone at room temperature enabled the cyclic species to be removed, since they are much more soluble than the linear ones[3]. However, the polydispersity, $\bar{M}_w/\bar{M}_n$, of this purified sample was higher than that of the other OSm_1 samples (see later) Two OSm_1 samples (OS31 and OS52) were obtained by isothermal fractional precipitation at 300K from a 1% w/v solution of DC 200/20 in methyl ethyl ketone using methanol as non-solvent. These had low polydispersities. Since the $\bar{M}_n$ values of the two OS31 samples isolated differently were sufficiently close to assign $m_1 = 31$ to each, the more polydisperse and hence atypical sample obtained via vacuum distillation is distinguished as OS31*.

In addition to n-alkanes extending up to $\mathrm{C_{44}H_{90}}$ of the purest grade available commercially, three additional OEm_2 samples all of nominal polydispersities of 1.1 and nominal molecular weights 700, 1000 and $2000\,\mathrm{g\,mol^{-1}}$ were obtained from Polymer Laboratories Ltd, Church Stretton, Shropshire, UK. They were dissolved in hot tetralin at 393K and precipitated in a fine, powdery form by dropwise addition of the solution to vigorously stirred methanol. The filtered, washed precipitate was dried *in vacuo* at 323K for 60 h.

Molecular weight and polydispersity

For all OSm_1 samples, $\bar{M}_n$ was measured by vapour pressure osmometry in toluene at 328K[1,2]. $\bar{M}_n$ ($= \bar{M}_w$)

0032-3861/83/111434-05$03.00

was taken as the formula molecular weight for the pure n-alkanes. $\bar{M}_n$ for OE24, OE35 and OE73 was measured by g.p.c. (RAPRA, Shawbury, Shropshire, UK, courtesy of Dr S. Holding), since the very high temperature (>*ca.* 393K) necessary for dissolution in tetralin precluded the use of vapour pressure osmometry for absolute determination. Similar considerations apply to the $\bar{M}_w$ values for these three samples.

For OS9, OS14, OS31*, OS31, OS52 and DC200/20, the values of $\bar{M}_w$ were measured via light scattering in toluene at 298K using a Sofica Model 42000 photometer with light of wavelength 436 nm *in vacuo*[2]. Extrapolation of the light-scattering plots to zero concentration of solute was effected over the linear region, i.e. below concentrations of 0.20 g cm^{-3}. With the same solvent, temperature and wavelength, specific refractive index increments (d*n*/d*c*) were measured with a Brice Phoenix differential refractometer, the values at zero oligomer concentration being −0.117, −0.112, −0.108 and −0.108 cm^3 g^{-1} for solutions of OS9, OS14, OS31* and DC200/20 respectively. Insufficiency of samples prevented similar direct measurements for OS31 and OS52, thus necessitating the following indirect procedure yielding specific refractive index increments of −0.106 and −0.105 cm^3 g^{-1} respectively. A linear dependence[4] of d*n*/d*c* on $1/\bar{M}_n$ was found for ten OSm_1 samples (see *Figure 1*). Consequently d*n*/d*c* could be interpolated from the measured $\bar{M}_n$ values of OS31 and OS52.

Polydispersities were obtained via g.p.c. and/or directly measured molecular weights.

Cloud point curves

Cloud point curves were established as before[1,5–7]. For each system about 15–22 different values of W_1 were obtained by successive small additions of OEm_2 to OSm_1 to cover the range W_1 = 0–0.99. The following 15 systems were studied in the present work:

OS4 + OE24; OS4 + OE35; OS4 + OE73;
OS6 + OE24; OS6 + OE35;
OS7 + OE24; OS7 + OE35;
OS14 + OE24;
OS31* + OE8; OS31* + OE13; OS31* + OE17;
OS31 + OE8; OS31 + OE17;
OS52 + OE8; OS52 + OE17.

RESULTS

Properties of the oligomers

The molecular weights and polydispersities of all the samples are listed in *Table 1*. As indicated, we have assumed $\bar{M}_w = \bar{M}_n$ = formula molecular weight for the pure n-alkanes. For the highest three oligoethylenes, $\bar{M}_w$, $\bar{M}_n$ and $\bar{M}_w/\bar{M}_n$ could be obtained only by g.p.c., the values lying in extremely good agreement with those quoted by the suppliers (who presumably also used g.p.c.).

Cloud point curves

Table 2 summarizes the results, which are categorized on the basis of three types (I, II and III) of phase separation curve. For the sake of making overall conclusions, results[1] appertaining to smaller values of m_1 and m_2 are also included in the Table. The general forms of the three types of curve are illustrated in *Figure 2*, where T_{m2} indicates the melting point of the OEm_2 species. Very little change in the cloud point temperature T_p at low W_1 is common to all types. This is followed at increasing W_1 by a continuous fall in T_p for type I or by a dome shape in type II or a double dome shape (i.e. bimodal form) in type III. Note that type II is subdivided according to whether the curve is symmetrical or unsymmetrical. At extremely high W_1 a shoulder appears in type III and in both forms of type II. Some cloud point curves are selected for more detailed discussion in the next section.

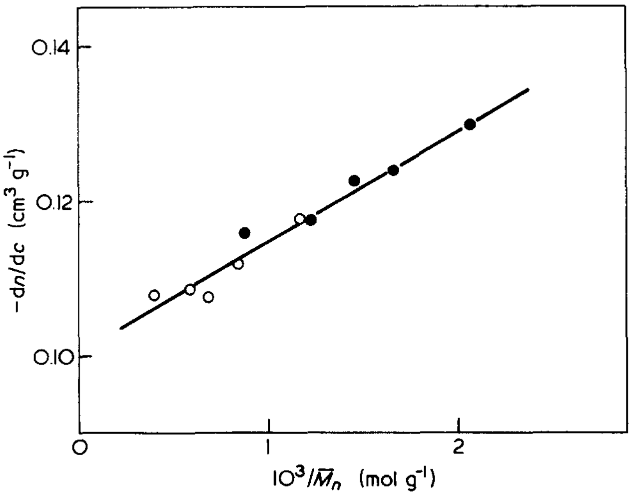

Figure 1 Variation of specific refractive index increment with reciprocal number average molecular weight for oligo(dimethyl siloxanes) in toluene at 298K and wavelength 436 nm. Present results (○) and earlier data[2] (●)

DISCUSSION

In the light of all the findings the following observations may be made:

(1) Type I obtains for the lowest molecular weight oligoethylene (OE8) irrespective of the chain length (m_1) of the oligo(dimethyl siloxane) with which it is mixed.

Table 1 Molecular weights and polydispersity of the oligomers

Sample	$\bar{M}_w$ (g mol^{-1})	$\bar{M}_n$ (g mol^{-1})	$\bar{M}_w/\bar{M}_n$	$\bar{M}_w/\bar{M}_n$ (via g.p.c.)
OS4	505	481	1.05	–
OS6	610	598	1.02	–
OS7	715	677	1.06	–
OS9	861	852	1.01	1.03
OS10	930	893	1.04	–
OS13	1180	1130	1.04	–
OS14	1250	1160	1.08	1.04
OS17	1470	1430	1.03	1.04
OS31*	3130	2420	1.29	1.23
OS31	2910	2530	1.15	1.13
OS52	4500	4060	1.11	1.17
DC 200/20	2860	1680	1.70	1.60
OE8[a]	254	254	1.00	–
OE13[a]	394	394	1.00	–
OE16[a]	478	478	1.00	–
OE17[a]	506	506	1.00	–
OE21[a]	618	618	1.00	–
OE24[b]	778	707		1.1
OE35[b]	1081	983		1.1
OE73[b]	2234	2031		1.1

[a] Values according to formula molecular weight for pure monodisperse n-alkanes
[b] Values via g.p.c. only

Table 2 Types of cloud point curve (I, II or III) observed for different combinations of OSm_1 with OEm_2

	OS4	OS6	OS7	OS9	OS10	OS13	OS14	OS17	DC 200/20 ($m_1 = 20$)	OS31*	OS31	OS52
OE8	I	I	I	I	I	I	–	I	I	I	I	I
OE13	I	I	I	–	I	I	–	–	III	III	–	–
OE16	I	I	I	–	I	I	–	–	III	–	–	–
OE17	I	–	–	I	–	–	II	II	III	III	II	II
OE21	I	I	–	II	II	–	II	II	–	–	–	–
OE24	II	II	II	–	–	–	II	–	–	–	–	–
OE35	II	II	II	–	–	–	–	–	–	–	–	–
OE73	II	–	–	–	–	–	–	–	–	–	–	–

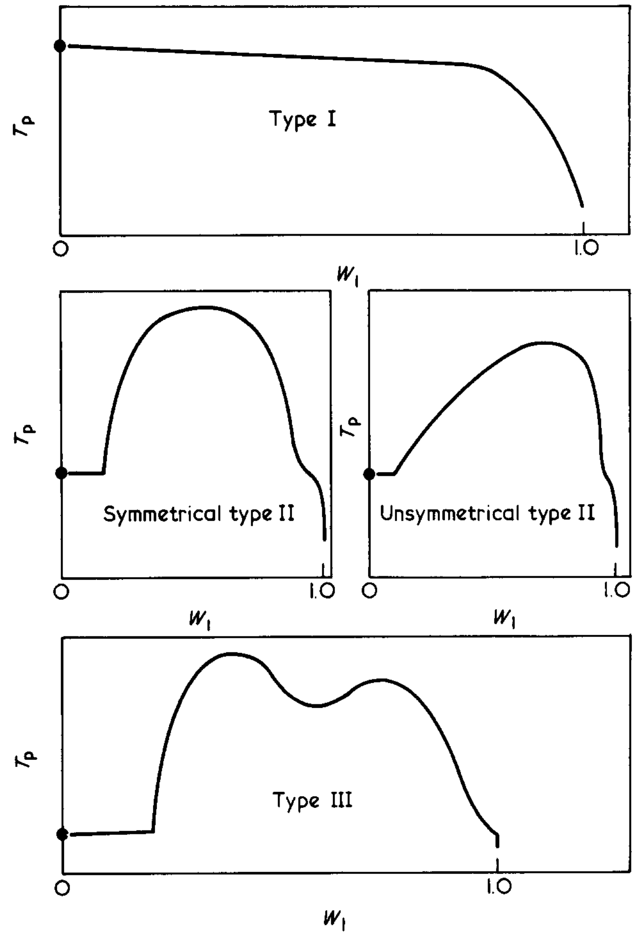

Figure 2 General forms of phase separation curve observed for mixtures of oligo(dimethyl siloxanes) (weight fraction W_1) with oligoethylenes. T_p is the phase separation temperature and T_{m2} (indicated by ●), is the melting point of the oligoethylene

(2) To obtain type II it is necessary that the chain length (m_1 or m_2) of only one of the components be large, in contrast with the earlier conclusion[1] that both m_1 and m_2 must be large.

(3) Regarding type II, those combinations in which $m_1 < 17$ and $m_2 \leqslant 21$ produce a symmetrical form, whereas an unsymetrical form obtains if $m_2 > 21$.

(4) The initial flat region of type II at low–moderate W_1 is illustrated in *Figures 3–5*. Curves for OE24 mixed with different OSm_1 species (*Figure 3*) all have the same temperature of 371K over this portion, which is the m.p. of OE24. A similar situation holds for *Figure 4*, where the flat regions coincide at the m.p. of the OE35, i.e. at 379K.

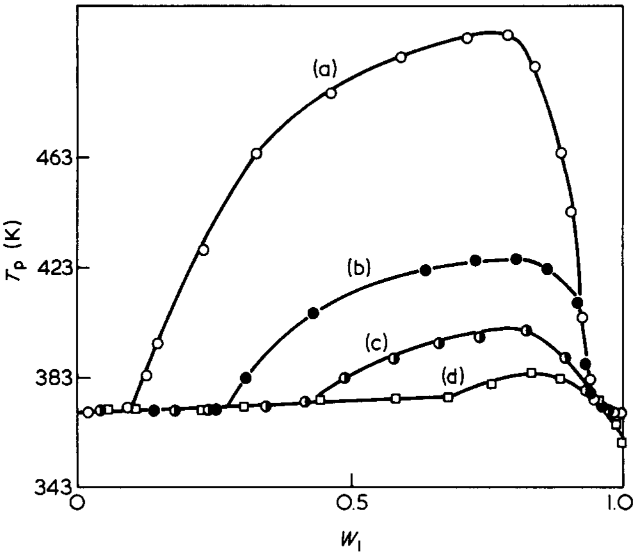

Figure 3 Cloud point curves for the mixtures (a) OS14/OE24, (b) OS7/OE24, (c) OS6/OE24 and (d) OS4/OE24

On the other hand, the flat regions occur at different temperatures for the systems in *Figure 5*. This is due to the use of a fixed OSm_1 with different OEm_2 species, the flat regions occurring at the melting point of the respective OEm_2 in each case (393K for OE73 and melting points previously mentioned for OE24 and OE35).

(5) *Figures 3–5* demonstrate that, with one component fixed (OSm_1 or OEm_2), the miscibility gap ΔW_1 at any temperature widens with increasing chain length of the other component (OEm_2 or OSm_1). Also the maximum T_p (i.e. the critical temperature T_{pc}) increases with increasing chain length of the other component. For example (*Figure 3*), in the system OE24/OS6 the maximum miscibility gap lies between $W_1 = 0.41$ and $W_1 = 0.94$ (i.e. $\Delta W_1 = 0.53$) and $T_{pc} = 400$K, whereas for OE24/OS7, $\Delta W_1 = 0.69$ and $T_{pc} = 426$K. Similarly (*Figure 5*) the maximum $\Delta W_1 = 0.30$ and $T_{pc} = 385$K for the system OS4/OE24, the corresponding values for OS4/OE35 being higher, viz. 0.59 and 443K respectively.

(6) At low W_1 the change in T_p is only small and the observed values of T_p seem more likely to represent crystallization or solubility temperatures. The true cloud point curve for liquid–liquid phase separation only becomes evident at higher values of W_1. After T_{pc} and subsequent fall in cloud point temperatures, the curve passes through T_{m2}. Here again crystallization is anticipated, but the flat region only assumes a shoulder due to

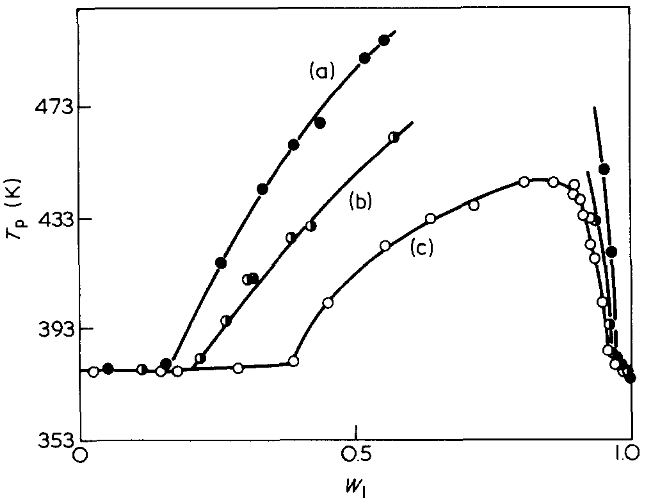

Figure 4 Cloud point curves for the mixtures (a) OS7/OE35, (b) OS6/OE35 and (c) OS4/OE35

the extremely low concentration of crystallizable material present, i.e. OEm_2 at its melting point.

Attention will be focused hereafter on the true cloud point regions of the curves.

The spinodal is defined[8–11] by $\partial^2\Delta G/\partial\phi_2^2=0$, which yields from the Flory–Huggins expression for the Gibbs free energy of mixing ΔG in terms of volume fraction ϕ, the following:

$$2g=(m_{w1}\phi_1)^{-1}+(m_{w2}\phi_2)^{-1} \tag{1}$$

$$2g_0=-6g''(1-2\phi_2)\phi_2-2g'(1-3\phi_2)+(m_{w1}\phi_1)^{-1}+(m_{w2}\phi_2)^{-1} \tag{2}$$

Here the subscript w signifies the weight average values of the chain lengths and, as before, the subscripts 1 and 2 relate to oligo(dimethyl siloxane) and oligoethylene respectively. The interaction parameter g (sometimes denoted also as χ) in equation (1) is constant at a particular temperature and independent of ϕ_2. In equation (2) a concentration dependence of the following form holds[8–11]:

$$g(T)=g_0+g'\phi_2+g''\phi_2^2 \tag{3}$$

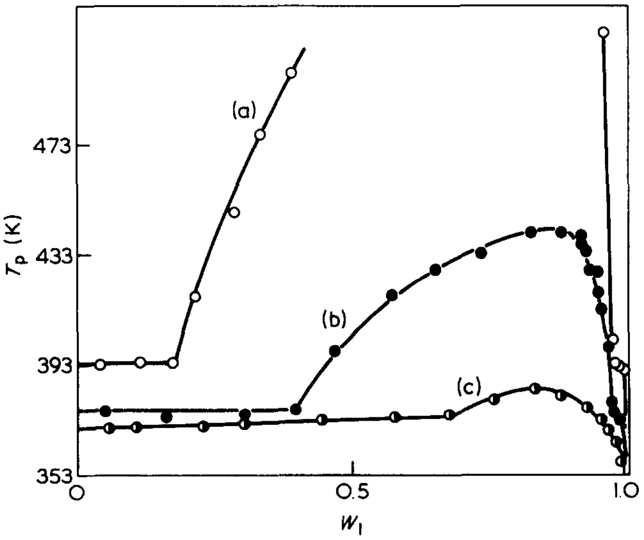

Figure 5 Cloud point curves for the mixtures (a) OS4/OE73, (b) OS4/OE35 and (c) OS4/OE24

At a temperature T_{pc} the critical point is defined[8–11] as $\partial^3\Delta G/\partial\phi_2^3=0$. When g is independent of ϕ_2, this yields equation (4), whilst equation (5) results if g is dependent on ϕ_2:

$$m_{z1}/m_{w1}^2\phi_{1c}^2=m_{z2}/m_{w2}^2\phi_{2c}^2 \tag{4}$$

$$6g''(1-4\phi_{2c})-6g'=m_{z1}/m_{w1}^2\phi_{1c}^2-m_{z2}/m_{w2}^2\phi_{2c}^2 \tag{5}$$

Here, subscript z signifies the z-average chain length and subscript c indicates composition at the critical point.

Since the spinodal and cloud point curves are of the same general form (although not exactly superimposable), it is possible to compare the shapes of the experimental curves with those calculated for the spinodal. In the calculated spinodal the calculated parameter is g, a decrease in this quantity corresponding with an increase of temperature in an experimental curve. Previously obtained symmetrical cloud point curves of type II were found to be capable of good simulation merely by assuming g to be independent of ϕ_2, i.e. by using equation (1). However in no instance was it possible to match the form of the present curves (all unsymmetrical type II) by this means. Assuming instead a concentration dependence of g (equation (3) in which the interaction parameters, but not the coefficients g' and g'', are temperature dependent[8]), g_0 was calculated via equation (2) for different compositions ϕ_2. The resultant curves shown in the upper part of *Figure 6* are seen to compare well in form with the corresponding experimental curves given in the lower part of *Figure 6*. The critical compositions ϕ_{1c} for these systems were calculated via equation (5) and are also indicated in *Figure 6*. These values are seen to be only very slightly higher than those for the experimental cloud point curves.

It should be noted that in these procedures it is necessary to assign appropriate values to g' and g'' in order to obtain the correct shape of the cloud point curve[8,9]. This can only be accomplished by trial and error. Thus $g'=0.10$ and $g''=0.05$ holds for the systems OS4/OE24, OS7/OE24 and OS14/OE24. As discussed elsewhere[1,8,9] the physical significance of the coefficients g' and g'' is still not fully resolved.

Selection of appropriate values of g' and g'' has been made to account for specific regions of experimental cloud point curves for other mixtures of oligomers. Thus, Koningsveld *et al.*[8] (see also Olabisi *et al.*[12]) were able to explain the shoulder at low W_1 observed by Allen *et al.*[5] for the system OSm_1/polyisobutene. A quadratic dependence of g on composition was also invoked by Koningsveld *et al.*[8] to account for the bimodality in mixtures of polyisoprene with polystyrene.

Type III behaviour is currently being analysed in more detail. Regarding type I, this is concluded to be exempt from consideration as a normal cloud point curve for polymer–polymer miscibility. Equilibrium can be regarded from different standpoints depending on which component is considered as solute and which as solvent. Thus, solubility and lowering of freezing (or melting) point of solvent are based on the chemical potentials of solute

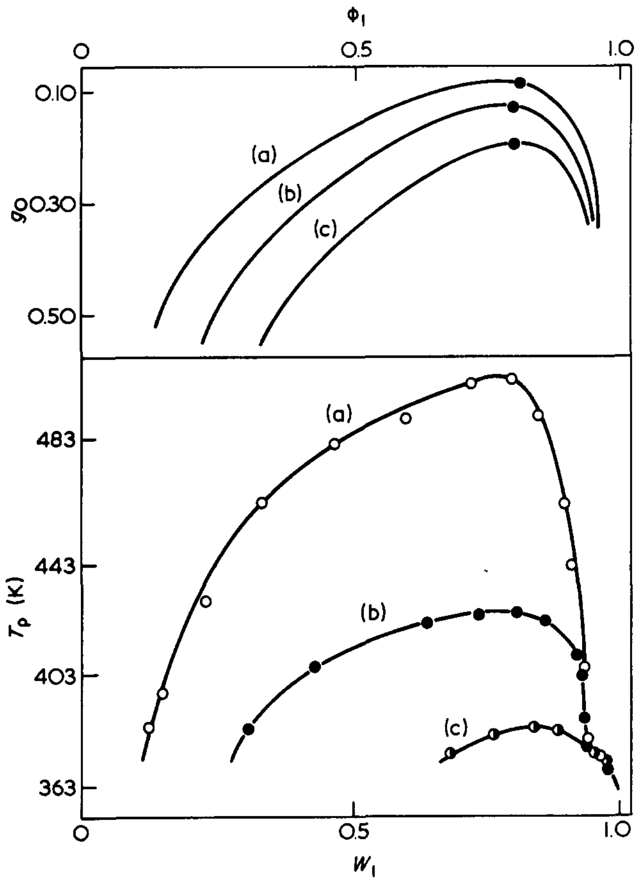

Figure 6 Spinodals calculated via equation (2) for the mixtures (a) OS14/OE24, (b) OS7/OE24 and (c) OS4/OE24. Appropriate values of *g'* and *g''* given in text. Lower three curves (a), (b) and (c) are the corresponding experimental cloud point curves. Critical compositions (●) calculated via equation (5)

and solvent respectively, but both yield expressions of the following ideal form[13]:

$$\ln x_2 = (\Delta H_{f2}/R)(T_{m2}^{-1} - T_p^{-1}) \qquad (6)$$

In the present context x_2 and ΔH_{f2} denote the mole fraction and molar enthalpy of fusion respectively of the OEm_2 and the observed T_p is to be interpreted as the solubility temperature. The validity of equation (6) has been verified[14] for the present type I systems by the linearity (between $W_1 = 0$ and $W_1 \approx 0.6$) in plots of $\ln x_2$ *versus* T_p^{-1} and good accord with accepted values for the quantities ΔH_{f2} and T_{m2} derived from the plots.

ACKNOWLEDGEMENTS

The provision of a maintenance grant (to I.M.I.) by Tun Dr Ismail Atomic Energy Centre, Bangi, Malaysia, is gratefully acknowledged.

REFERENCES

1 Huglin, M. B., Idris, I. M. and Sokro, M. B. *Makromol. Chem. Rapid Commun.* 1981, **2**, 17
2 Huglin, M. B. and Sokro, M. B. *Polymer* 1980, **21**, 651
3 Dodgson, K. and Semlyen, J. A. *Polymer* 1977, **18**, 1265
4 Huglin, M. B. in 'Light Scattering from Polymer Solutions' (Ed. M. B. Huglin), Academic Press, London, 1972, Ch. 6
5 Allen, G., Gee, G. and Nicholson, J. P. *Polymer* 1961, **2**, 8
6 Wolf, B. A. and Blaum, G. *J. Polym. Sci., Polym. Symp. Edn.* 1977, **61**, 251
7 Wolf, B. A. and Blaum, G. *Makromol. Chem.* 1979, **180**, 2591
8 Koningsveld, R., Kleintjens, L. A. and Schloffeleers, H. M. *Pure Appl. Chem.* 1974, **39**, 1
9 Koningsveld, R. and Kleintjens, L. A. *Br. Polym. J.* 1977, **9**, 212
10 Koningsveld, R. and Kleintjens, L. A. *J. Polym. Sci., Polym. Symp. Edn.* 1977, **61**, 221
11 Koningsveld, R., Kleintjens, L. A. and Shultz, A. R. *J. Polym. Sci. A-2* 1970, **8**, 1261
12 Olabisi, O., Robeson, L. M. and Shaw, M. T. 'Polymer–Polymer Miscibility', Academic Press, London, 1979, Ch. 2
13 Castellan, G. W. 'Physical Chemistry', Addison-Wesley, London, 1964, p. 259
14 Sokro, M. B. Ph.D. Thesis, University of Salford, 1980